Approved for Public Release: 11-3322.
Published in the "Proceedings of the 24th International Technical Meeting of The Satellite Division of the Institute of Navigation (ION GNSS 2011)".

Electro-Textile Ground Planes for Multipath and Interference Mitigation in GNSS Antennas Covering 1.1 to 1.6 GHz

B. Rama Rao, E. N. Rosario
The MITRE Corporation
Bedford, Massachusetts

Biography:

B. Rama Rao is a Principal Engineer at The MITRE Corporation. He had received his Ph.D. degree in Applied Physics from Harvard University. Prior to joining MITRE, he held technical staff positions at the Sperry Research Center and M.I.T. Lincoln Laboratory. He was also an Assistant Professor of Applied Physics at Harvard University and a Research Associate at M.I.T. He holds 10 U.S. patents, three of which are on GPS antennas.

Eddie N. Rosario is a member of the technical support staff in the Sensors and Electromagnetics Systems department at The MITRE Corporation in Bedford, Massachusetts. He helps in the design and in the measurement of antennas needed for a wide variety of projects using The MITRE Corporation's Near Field and Far-Field Antenna Test Ranges.

Abstract:

This paper deals with the design of new types of ground planes made from low cost, lightweight, and flexible electro-textiles that suppress both edge and curved surface diffraction effects that can degrade the radiation pattern of GNSS antennas. Two of these are very thin, resistivity tapered textile ground planes that are ultra wideband and able to operate from 1.1 to 1.6 GHz. Their resistivity profile has been specifically designed to suppress edge diffraction effects; their wide bandwidth makes them particularly suitable for use with multiband GNSS antennas. This ground plane can be sandwiched between plastic cover sheets for weather protection. The second type is a conformal ground plane designed to suppress curved surface diffraction that affects GNSS antennas used in avionics. It operates as a frequency selective surface with Electronic Band Gap (EBG) characteristics and is able to attenuate antenna backlobes caused by curved surface diffraction from the fuselage of an aircraft. It is designed to operate only over a specific band of frequencies and is very effective when used in conjunction with a "Reduced Surface Wave (RSW)" antenna consisting of an annular ring microstrip patch antenna whose inner periphery is connected to the fuselage of the aircraft. The RSW antenna is also made from electro-textiles. The performance this antenna when used with the EBG ground plane has been validated through measurements on a large diameter metal cylinder which simulates the fuselage of an aircraft. The results of these measurements, performed in the GPS L_1 band, indicate that when used together they are able to suppress almost all of the antenna backlobe radiation below the horizon. This is an enhancement above the body masking capability of the aircraft fuselage and provides improved

protection to the GPS antenna from multipath and interference, especially co-site interference from other antennas located on the belly of the aircraft

Introduction

The radiation patterns of GNSS antennas used in commercial and military navigation systems are affected by diffraction from either the edges of a planar metal ground plane or from curved surface diffraction generated by “creeping waves” that radiate energy as they propagate around the fuselage of an aircraft. These diffraction effects cause antenna backlobes that make the antenna susceptible to interference and multipath; they can also cause other phase anomalies that degrade the accuracy of high precision GNSS measurements. GNSS antennas are required to have very wide beams necessary to capture low elevation satellites needed for good PDOP (Position Dilution of Precision). They can, therefore, cause a significant illumination of the platforms on which they are located enhancing these diffraction effects. This paper will describe two types of thin, lightweight and flexible resistivity tapered ground planes made from electro-textiles that offer a low cost, potentially easy to install (?), and broadband solution for mitigation of antenna backlobes and pattern distortions created by these diffraction effects. In addition, we have taken advantage of the flexibility and lightweight properties of these electro-textiles to design a conformal Electronic Band Gap (EBG) ground planes that can be wrapped around the cylindrical fuselage of an aircraft to suppress diffraction backlobes. Experiments have been conducted with an antenna mounted on a 5" cylinder that is 5' in diameter to demonstrate the efficacy of these ground planes for suppressing backlobes generated by an antenna mounted on a metal cylinder that is 5' in diameter for simulating the effects on an aircraft fuselage.

Analysis and Verification of Diffraction Effects and Their Impact on GNSS Antennas

The edge diffraction effects generated by a GPS microstrip patch antenna placed at the center of a rectangular metal ground plane is illustrated in Figure 1; the measured antenna pattern at a frequency of 1.5754 GHz for a patch antenna placed on 48" square ground plane is shown in Figure 2. The antenna backlobes shown in this figure are due to diffraction from the edges of this ground plane. In addition, the radiated and edge diffracted signals also interact at higher elevations to cause amplitude and phase ripples in the antenna pattern that are clearly visible. This is called “speckle multipath” and can affect the accuracy of carrier phase measurements used in high precision GPS such as surveying and other types of geodetic measurements.

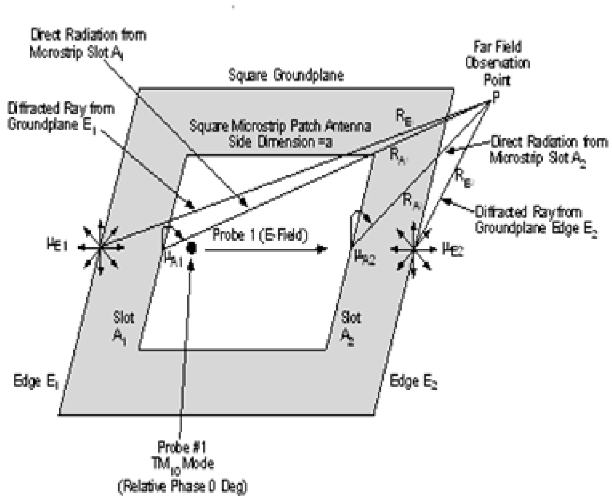

Figure 1(a). Edge Diffraction Effects from a Metal Ground Plane on the Radiation Pattern of a Patch Antenna

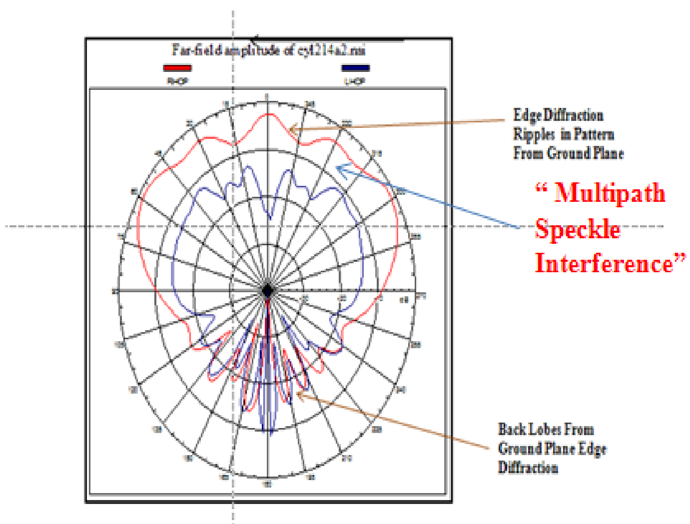

Figure 1(b). Measured Pattern of a Patch Antenna on Metal Ground Plane

Curved surface diffraction occurs in GPS antennas located on top of a cylindrical shape fuselage of an aircraft are illustrated in Figure 2. As shown in Figure 2(a) on the right, the surface waves generated by the GPS antenna propagate along a geodesic patch around the smooth metallic surface of the aircraft fuselage. While propagating around this curved surface they also shed energy at each point of tangency to the curved metal surface, resulting in the generation of a large back lobe in the "shadow" region of the aircraft. Figure 2(b) shown on the left side illustrates an additional diffraction effect caused by airborne antennas – this is contributed by edge diffraction from the wings. The measured roll plane patterns for vertical polarization component of the electric field E_ϕ and horizontal polarization component of the electric field E_θ of a GPS antenna located on a 1/10 scale model of a C-12J aircraft are shown on the right side of Figure 3. A picture of this aircraft is shown in the central left portion of this figure; a picture of the 1/10 scale model of the aircraft that was used for measuring the antenna patterns as also shown at the far left of the figure. The amplitude of these backlobes has also been accurately predicted through EM modeling as shown in the figure on the right of Figure 3; the theory predicts that these backlobes are caused by curved surface diffraction [3] from the fuselage of the aircraft. In addition, there are also edge diffraction caused by the wings and other appendages on the aircraft as shown in Figure 2(b). These backlobes make the aircraft GNSS antenna vulnerable to interference from ground based interference sources as well as from co-site interference from signals radiated by other antennas co-located on board the aircraft. A typical is the harmonics from UHF and VHF antennas or radiation from L band antennas on the aircraft.

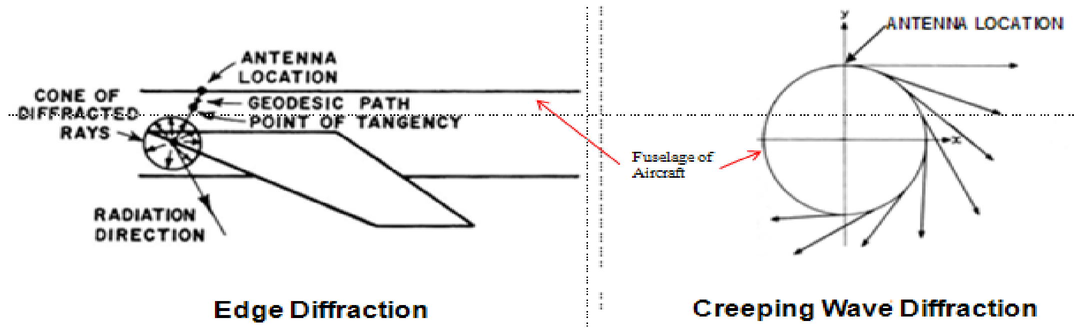

Figure 2(b) **Figure 2(a)**

Figure 2. Curved Surface ("Creeping Wave") Diffraction and Edge Diffraction Effects from GNSS Antenna on Top of Aircraft

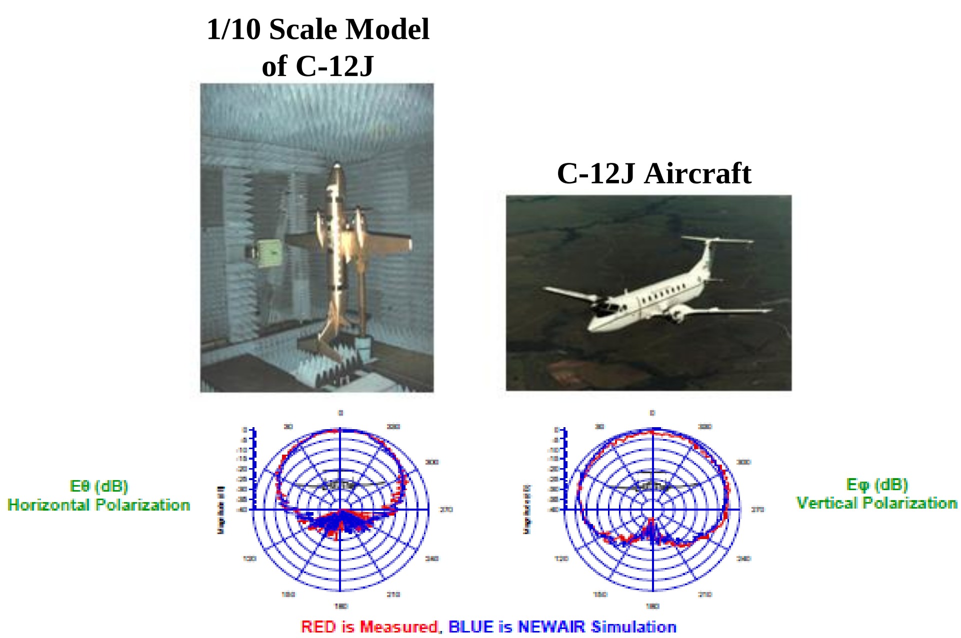

Figure 3. Scale Model Measurement of the Effects of Diffraction from the Curved Surface of the Fuselage on the Radiation Pattern of a Patch Antenna on a C-12J Aircraft [From Reference 1]

The imminent emergence of four new global navigation systems: Modernized GPS, Galileo, GLONASS, and Compass as well as other SBAS systems has generated strong interest in new types of ground planes which when used with wideband antennas can suppress multipath over the entire GNSS band from 1.1 to 1.6 GHz allowing multiband measurements to improve navigational precision and satellite availability and also allow fast ambiguity resolution. Several new types of broadband ground planes have recently been proposed. These include Novatel's GNSS-750 hemispherical choke ring ground plane, new types of frequency selective cut-off choke ring ground planes, Electronic Band Gap (EBG) and Artificial Magnetic Conductor (AMC) Ground planes and resistivity tapered ground planes made by the Trimble Corp. However some of these ground planes, such as choke ring ground planes or EBG ground planes, are large, heavy, expensive, inflexible and not suitable for use in compact, portable systems or on aircraft. Many such designs are also limited by bandwidth and cannot cover the entire GNSS band.

In this paper, we have designed and tested two new types of planar resistivity tapered, ultra-broadband ground planes that are made entirely from electro-textiles; especially new resistive textiles manufactured by the Eeonyx Corporation [2]. These Eeonyx textiles are made from fibers which have coatings whose surface resistivity can vary from 5 to 10^9 ohms per square. This enables the manufacture of textiles with graduated resistance as well as patterned coatings of complex shapes allowing a variety of ground plane designs especially suitable for GNSS applications. Some of these resistive coatings are insoluble in water, concentrated acids and organic solvents. They also display good long-term stability under ambient air and prolonged exposure to UV. Further protection against environmental effects can be achieved by "sandwiching" these textile ground planes between two thin plastic cover sheets. Earlier work on resistive ground planes for GPS applications was conducted by The MITRE Corporation and presented at the 1998 PLANS Conference [3]. In this earlier effort the resistive ground planes were made from Indium Tin Oxide sputtered on Kapton films; the long-term environmental stability of these resistive films, which are prone to oxidation, are not as good as the electro-textiles used in this current effort.

Wideband Resistivity Tapered Planar E-textile Ground Planes

Edge diffraction effects in ground planes can be reduced by the use of resistivity tapering where the surface resistivity gradually increases from the center to the edge of the ground plane. The amplitude of the surface waves generated by the antenna is gradually reduced as they propagate radially outward resulting in negligible diffraction once they reach the edge. Both types of ground planes that were built were made from the Eeonyx electro-textile materials and are very light in weight, inexpensive and wideband to cover all GNSS frequencies from 1.14 to 1.65 GHz. The reason for this wide bandwidth is they do not need require concentric circular grooves that are specifically tailored to certain frequency bands as in choke ring ground planes; nor is their operation restricted in frequency by the geometrical periodicity of these surfaces and resonant cell structures needed by the EBG ground planes [4]. Two types of E textile ground planes using exponential and step tapering have been investigated and their performance over the entire GNSS band has been measured. The radiation pattern of a wideband GNSS antenna, Model Number DMC-146-24-1 made by EDO, placed at the center of these ground planes was used as the test antenna. These results have been compared against that obtained by placing the same antenna at the center of a conventional planar metal ground plane as well as on a Novatel GNSS 750 choke ring ground plane. The performance of these electro-textile ground planes were also tested by measuring the elevation plane patterns on other MITRE designed wideband GNSS antennas.

Exponentially Tapered 26" Square E-textile Ground Plane:

Figure 4(a) shows a picture of a 26" square, exponentially tapered E-textile ground plane whose resistivity profile is shown in Figure 4(b). The central 6" wide section of this ground plane is made from a perfectly conducting textile, but the resistivity of the bordering 7" section has a steep exponential taper. The surface resistivity increases from0 ohms/square starting at 7" to 2000 ohms square at 12". It was prepared for MITRE by the Eeonyx Corporation using their special resistive fabrics. The GNSS antenna shown at the center of this ground plane is the EDO Model DMC-146-24-1 which has a very wide bandwidth that covers the entire GNSS band.

26" Wide Resistivity Tapered E-Textile Ground Plane

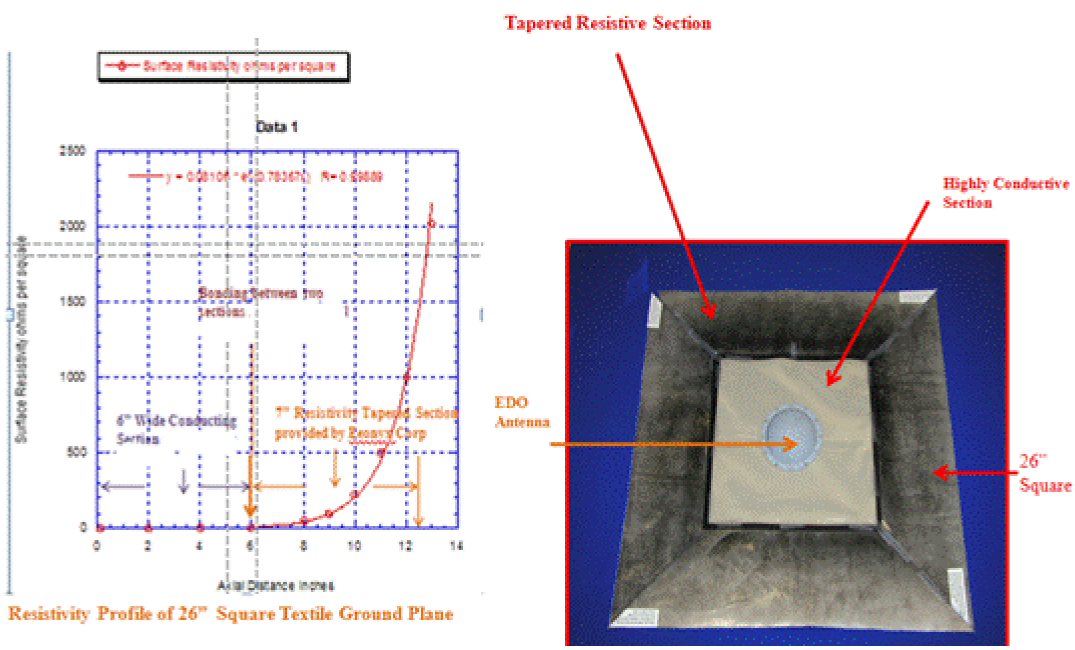

4(b) 4(a)

Figure 4. E-textile Ground Plane with Exponentially Tapered Resistivity

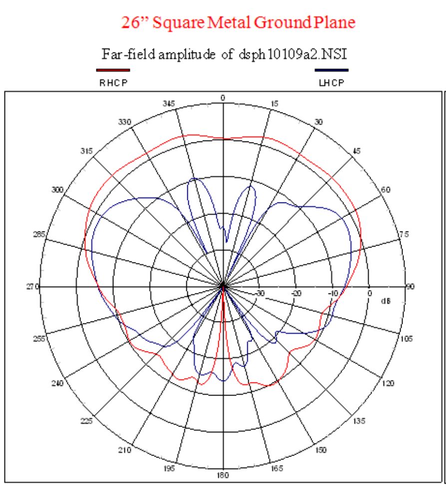

Figure 5(a)

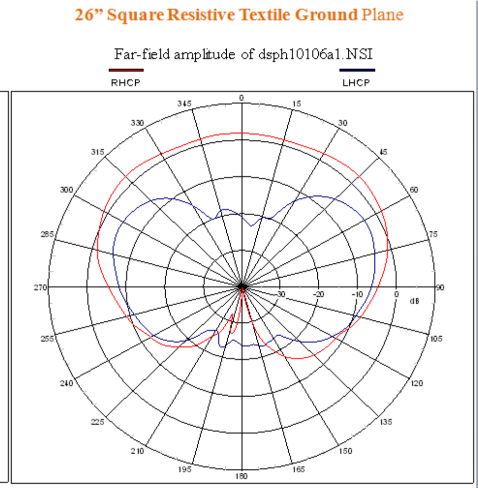

Figure 5(b)

Curves in Red are RHCP

Curves in Blue are LHCP

Figure 5. Comparison of Measured Elevation Plane Patterns of the EDO Antenna on 26" Square Planar Metal Ground Plane [shown in Figure 5(a)] and the 26" Square Textile Ground Plane with Exponential Resistivity Tapering [shown in Figure 5(b)]

The measured elevation plane pattern of the EDO antenna placed at the center of a 26" square metal ground plane is shown in Figure 5(a) on the left of the above figure. Figure 5(b) on the right shows the pattern when the same EDO antenna is placed at the center of a 26" exponentially tapered textile ground plane. Notice the suppression of the backlobes for both RHCP and LHCP polarizations at the lower elevation angles below the horizon for the resistivity tapered ground plane and also absence of any ripple at higher elevation angles.

Figure 6(a) shows the elevation plane pattern measured at 1.5754 GHz for the EDO antenna when placed on the NovAtel GNSS 750 3D choke ring ground plane. The NovAtel ground plane is 15" in diameter with a height of 7.9"; it weighs 16.75 pounds. Figure 6(b) shows the corresponding measured elevation plane pattern when the same antenna is placed at the center of the 26" exponentially tapered resistive textile ground plane. Note the good backlobe suppression for both polarizations by both types of ground planes. Figure 6 shows the performance of this resistivity tapered ground plane across the entire GNSS band from 1.164 GHz, the lower end of the GPS L_5 and the Galileo’s E5b band, to 1.606 GHz – the upper band frequency of the GLONASS L1 (or G1) band. Measurements made at other intermediate frequencies 1.2276 GHz, the center frequency of the GPS L_2 band and 1.5754 GHz, the center frequencies of the GPS L_1 band. Hence, the suitability of this ground plane for operation of all major GNSS systems: Modernized GPS, Galileo, Beidou and GLONASS has been demonstrated in these measurements. An even smaller textile ground plane that is only 14" square, but with a resistivity step taper will be discussed next. Its performance is comparable to that of the larger exponentially tapered ground plane.

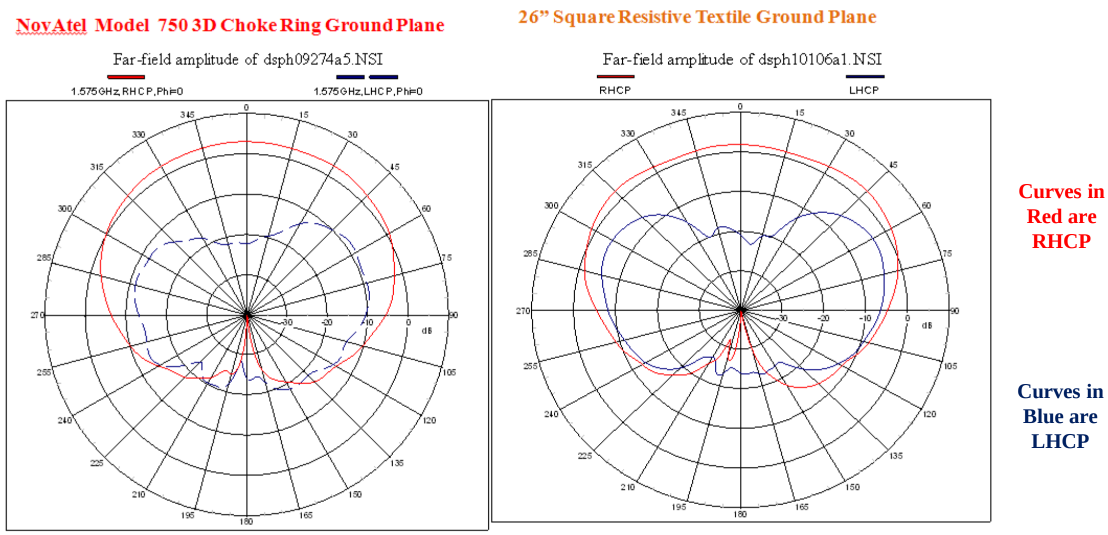

Figure 6(a) **Figure 6(b)**

Figure 6. Comparison of Measured Elevation Plane Patterns of a EDO Antenna Placed on NovAtel's 3D Choke Ring Ground Plane [shown in Figure 6(a)] with the 26" Square Textile Ground Plane with Exponential Resistivity Tapering [shown in Figure 6(b)]

Figure 7 shows the wide band characteristics of the 26" resistivity tapered ground plane; the elevation plane patterns were measured at four different GNSS frequencies covering the GNSS band.

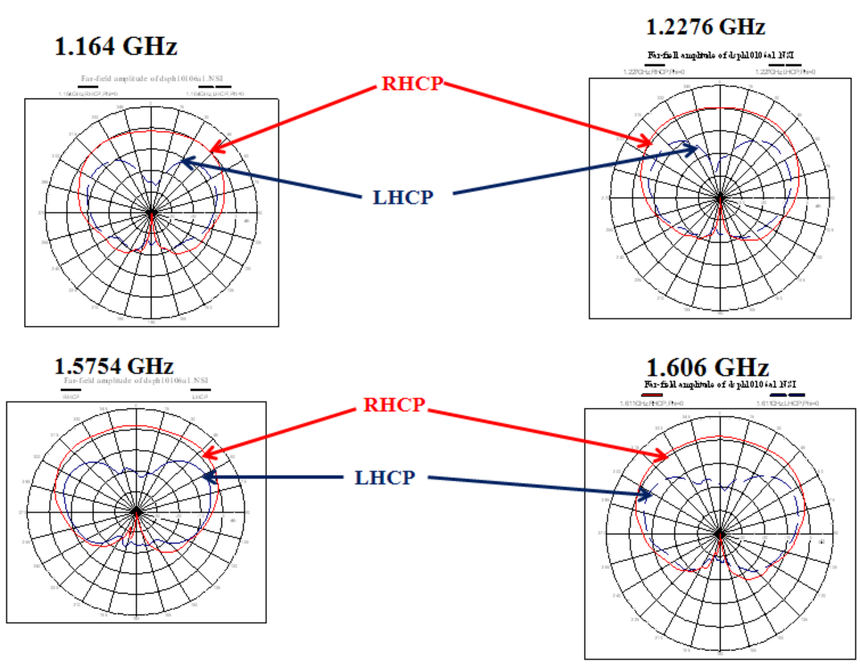

Figure 7. Measured Elevation Plane Patterns of the 26" Resistivity Tapered E-textile Ground Plane at Four Different Frequencies Covering the Entire GNSS Band

Step Tapered 14" Square Electro-Textile Ground Plane

Figure 8 shows a picture of the 14" wide step tapered E-textile ground plane. The central 7" square section is made of a conducting textile material; the peripheral 3.5" border section on all sides of this central portion has a step tapered resistive textile section made from textiles of different widths and resistivity. The innermost section closest to the central conductive section is 1.25" wide with a surface resistivity of 20 ohms/square; followed by 0.90" wide section with a resistivity of 100 ohms/square, a 0.84" wide section with a resistivity of 500 ohms/square and final edge section of 0.50" with a resistivity of 1000 ohms/square.

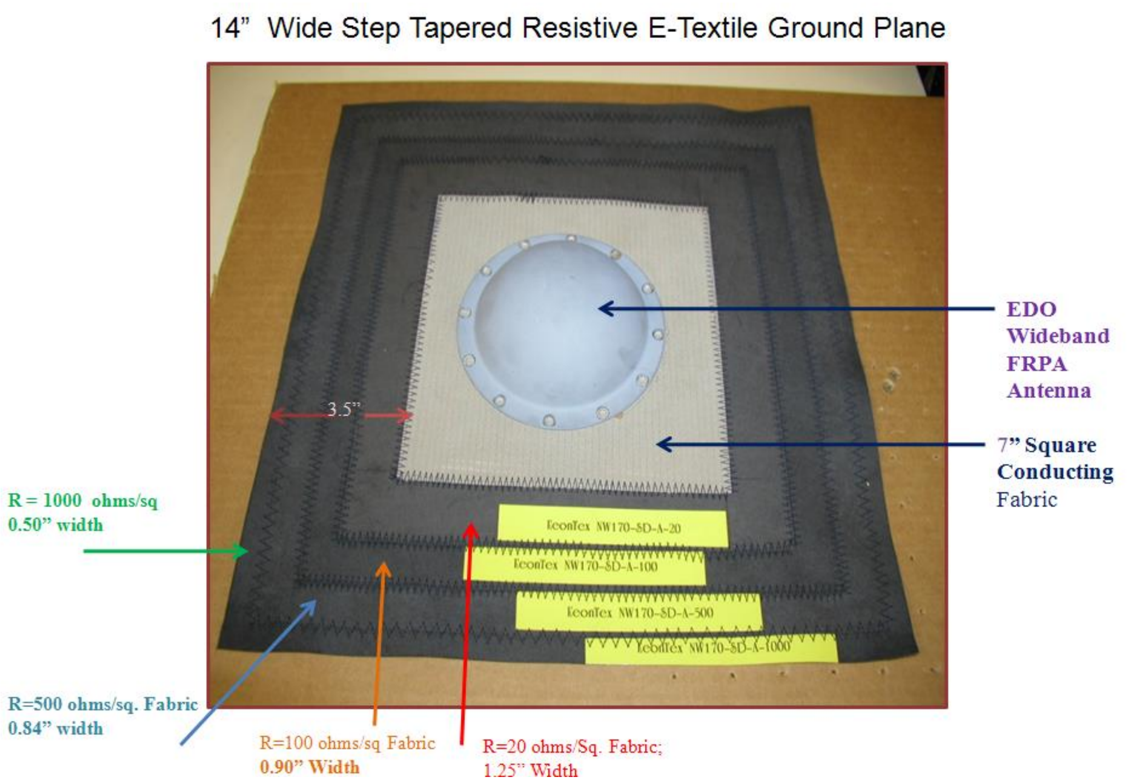

Figure 8. Picture of the 14" Square E-textile Ground Plane with Step Resistivity Tapering

Figure 9 shows the comparison of the elevation patterns of a EDO antenna when placed at the center of the 14" wide step tapered, resistive E-textile ground plane (as shown in Figure 8) and at the center of the exponentially tapered resistive ground plane (as shown in the earlier Figure 4(a). The patterns were measured at 1.164 GHz, the low end of the GNSS frequency band and at 1.611 GHz, which is well above the maximum GNSS frequency band. These measured patterns indicate good suppression of backlobes and no ripples in the pattern at the higher elevation angles; it demonstrates that both types of ground planes have sufficient bandwidth to cover the entire GNSS frequency band.

Comparison of 26" and 14"Restive Textile Ground Planes at other GNSS frequencies
(1.164 GHz & 1.611 GHz)

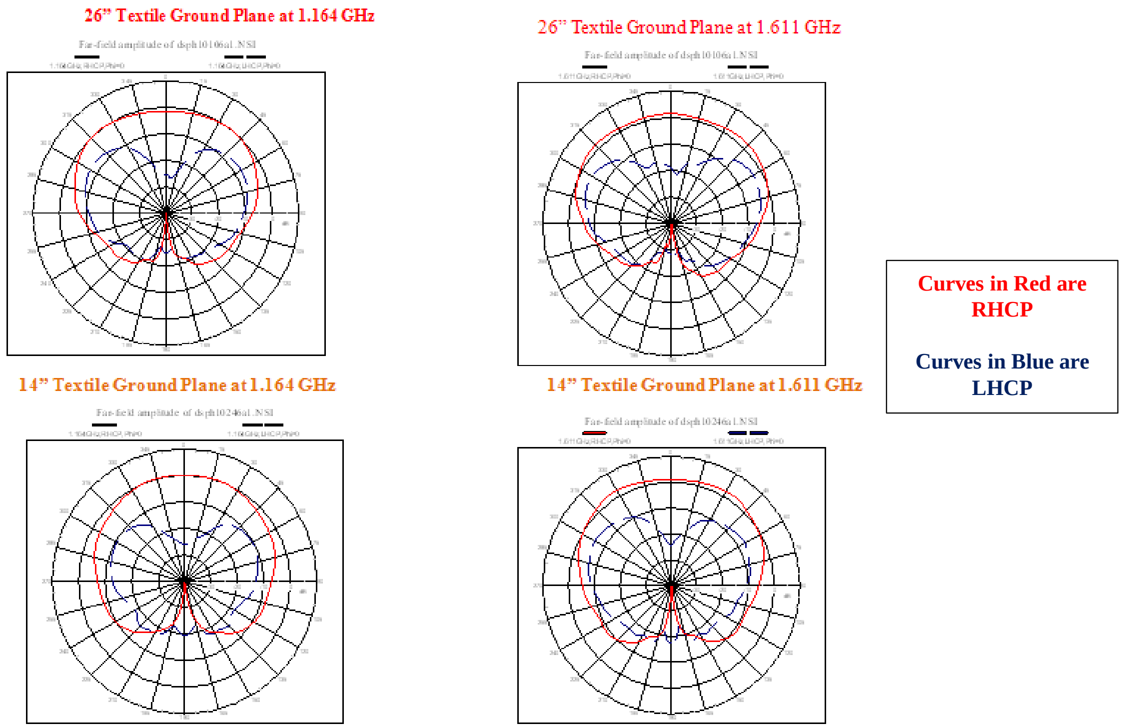

Figure 9. Comparison of the Measured Elevation Plane Patterns of the 26" and 14" E-textile Ground Planes at 1.164 GHz and 1.611 GHz

The two types of resistivity tapered textile ground planes described above cannot be placed in direct contact with an underlying metal surface since this will degrade their ability to suppress surface waves by affecting their resistance. They can instead be mechanically supported on plastic, non-conducting surfaces placed underneath them; sandwiching them between two plastic cover sheets will provide an extra benefit of the protecting the textile ground plane against adverse weather conditions such as rain.

Evaluation of Ground Plane Performance in Terms of Multi-Path Ratio (MPR) and Phase Center Variations

The ability of these ground planes to reject multipath signals can be gauged in terms of two performance metrics: 1) the Multi-Path Ratio (MPR) and the Front-to-Back Ratio (FBR), also sometimes called the Up/Down ratio and 2) Phase Center Variations with respect to elevation angle.

Figure 10 is an illustration of the multipath reflected signals received by the GNSS antenna.

MPR and FBR are defined terms of the variation in the antenna gain as a function of the elevation angle for the right-hand circular polarization (RHCP) and the left-hand circular polarization (LHCP) radiated signals – these represent the principal and cross polarized signals from the antenna.

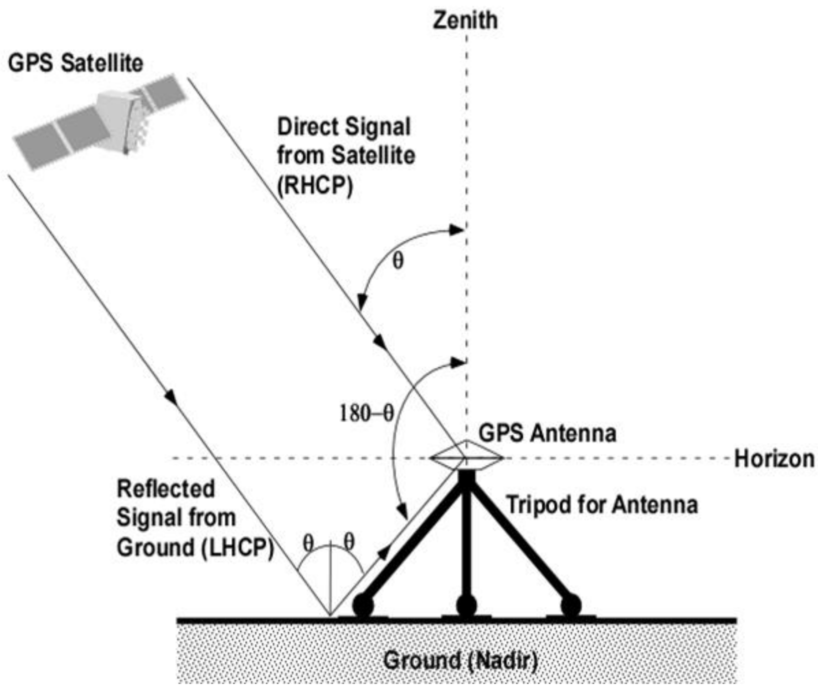

Figure 10. Diagram Illustrating Multipath Reflected Signals Received by a GNSS Antenna

The Multipath Ratio (MPR) is defined by the equation:

$$MPR = \frac{G_{RHCP}(\theta)}{G_{RHCP}(180-\theta) + G_{LHCP}(180-\theta)}$$

It is the ratio of the radiation of the principal polarization in the upper hemisphere where the satellite signals are received by the antenna to the total radiation from both polarizations in the lower hemisphere where multipath and interference signals are most prevalent.

The Front-to-Back Ratio (FBR) is defined as

$$FBR = \frac{G_{RHCP}(\theta)}{G_{LHCP}(180-\theta)}$$

Sometimes the FBR is just restricted to the zenith angle $\theta = 0°$ in the numerator and to nadir angle $\theta = 180°$ in the denominator. Note that the principal polarization in the upper hemisphere is RHCP; however, the polarization of the strongest multipath signal after a single bounce at a perfectly conducting surface is LHCP.

Hence,

$$FBR = \frac{G_{RHCP}(\theta = 0^{\circ})}{G_{LHCP}(\theta = 180^{\circ})}$$

The second performance metric to evaluate ground plane performance is by considering Phase Center Variation (PCV) as a function of elevation and azimuth angles and also with frequency.

$$\Delta_{PCV} = d\tau(\theta, \phi, f) \cdot \left(\frac{\lambda}{360^{\circ}} \right)$$

In the above equation, Δ_{PCV} = Range Correction due to the Phase Center Variation and $d\tau(\theta,\phi,f)$ is the Phase Center Variation in degrees which is a function of the elevation and azimuth angles and also frequency.

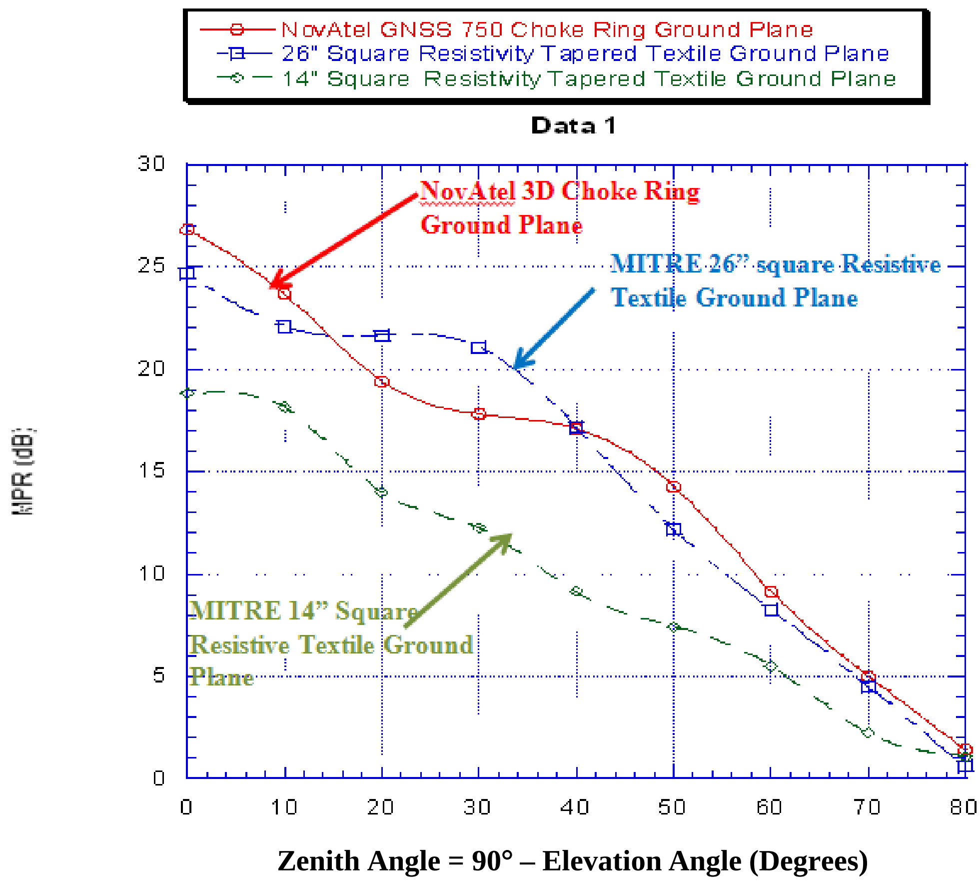

Figure 11. Comparison of Measured Multipath Ratio (MPR) as a Function of Zenith Angle = 90° – Elevation Angle at 1.5754 GHz for Three Different Ground Planes

A comparison of the variation in MPR versus elevation angle for the three different ground planes – the MITRE 26" and 14" resistive textile ground planes and the Novatel 750 3D choke ring ground plane are shown in Figure 11. The results shown in this figure indicate the MPR for the 26" textile ground plane with exponentially tapered resistivity is comparable to the Novatel 3D choke ring ground plane.

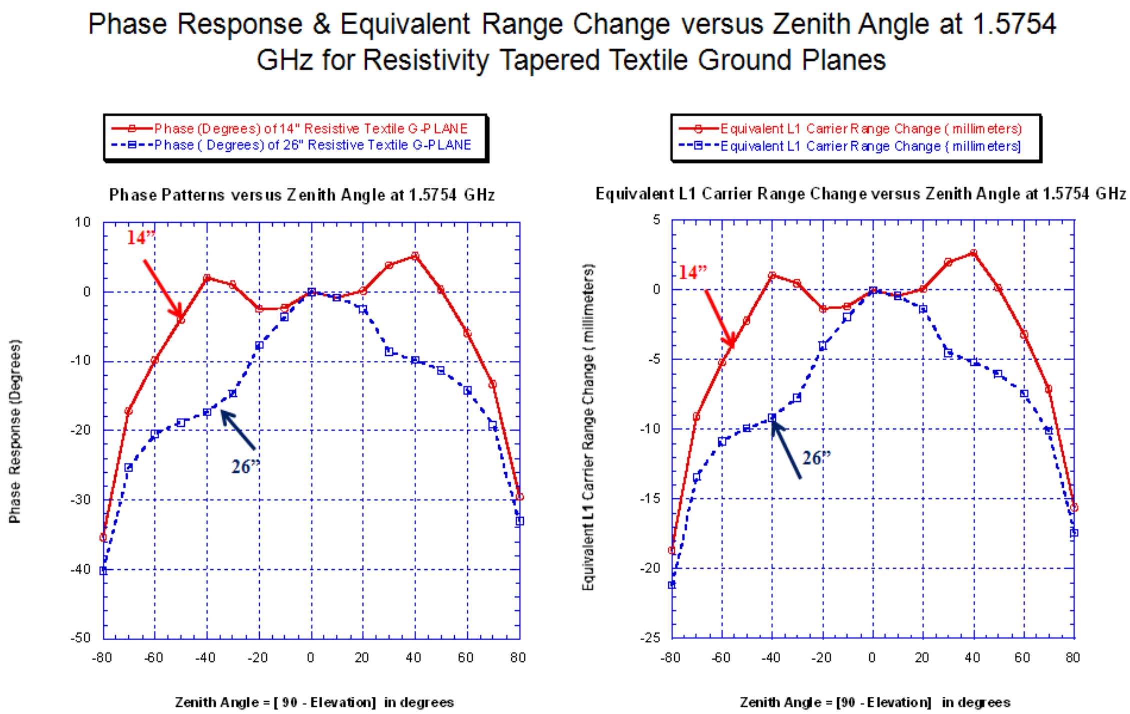

Figure 12. Phase Response & Equivalent Range Change versus Zenith Angle = 90° – Elevation Angle at 1.5754 GHz for 26" and 14" Square Resistivity Tapered Ground Planes

Figure 12 shows the variation in the measured phase response and the corresponding equivalent range correction versus elevation angle for the 26" and 14" resistive textile ground planes; these measurements were made at 1.5754 GHz. Results indicate that the 14" square resistivity tapered ground plane shows less than 10° of phase variation over a ±60° variation in the zenith angle – or for elevation angles varying from 30° to 90°. This represents an equivalent carrier range change of ±10 millimeters relative to measurements at zenith. The corresponding phase variation over ±75° variation in zenith angle – or for elevation angles varying from 15° to 90° is less than 22°. This corresponds to a carrier range change of ±15 millimeters. The 26" square ground plane with an exponential tapering in resistivity shows a larger variation in both phase variation and carrier range change over this same range of elevation angles as shown in this figure. This indicates that a steeper step gradient in resistivity over a shorter 3.5" length is more effective in reducing phase variation than a more gradual exponential taper over a 7" length.

Conformal Electronic Band Gap (EBG) Textile Ground Plane for Suppression of Curved Surface Diffraction Effects on GPS Aircraft Antennas

Resistive textile ground planes described above do not work well when placed directly on the fuselage of aircraft. The aircraft fuselage which is metallic adversely affects the ability of these ground planes to suppress surface waves by altering their resistive properties. Hence, a conformal Electronic Band Gap (EBG) ground plane made entirely from electro-textiles has been designed specifically for avionics applications. The "metamaterial" that is used to build this EBG ground plane is realized by placing periodic resonant metal structures on top of a dielectric substrate. It presents very high impedance to surface waves propagating on the surface of the fuselage of the aircraft which is represented by the large metal cylinder used in these investigations. Based on the design first proposed by Sievenpiper [4]; it has since been investigated by other authors [5] and has also been applied for improvement of GNSS antenna performance [6,7]. Figure 13 shows a picture of a 14" square EBG textile ground plane with an EDO antenna placed at its center.

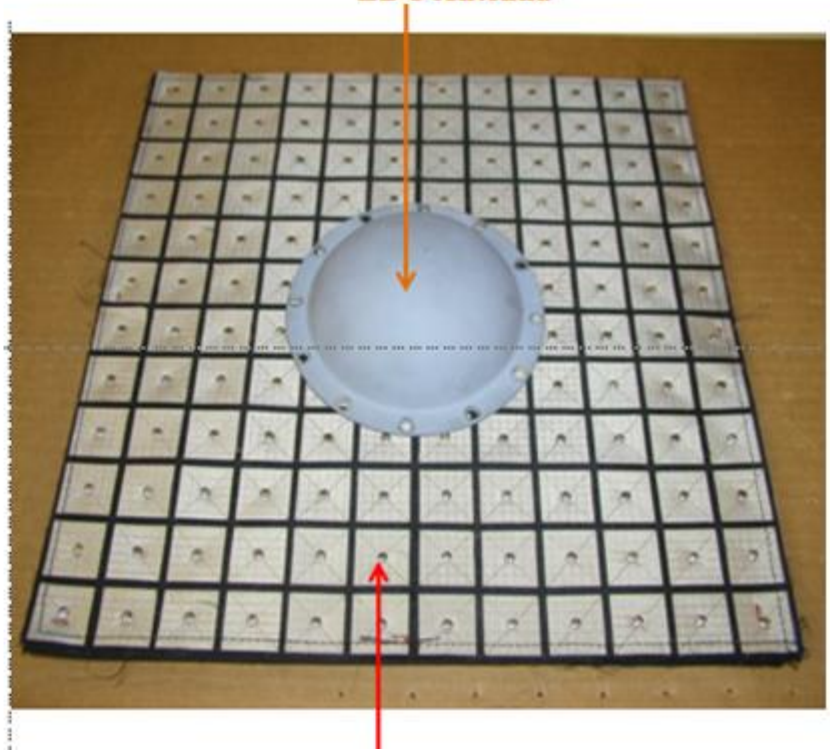

Figure 13. Flexible "Electronic Band Gap (EBG)" Ground Plane for Suppression of Curved Surface Diffraction from GPS Antennas on Aircraft

This EBG ground plane consists of three distinct layers; the top layer is a two dimensional periodic array of square shaped conducting patches made from a conducting electro-textiles. Directly below this periodic array of conducting patches are several layers of non-conducting textiles which serve as the dielectric substrate. The textile material used for this layer was made from Cordura fabric with a dielectric constant of 1.83; its dielectric constant was measured with a microstrip ring resonator. The third layer is made from a perfectly conducting textile material; which now serves as the bottom ground plane of this frequency selective surface. At the center of each of the conductive square patches in the top layer is a “conducting via” or metal post that connects the patch to the bottom ground plane. Thin metal screws were used to serve as these “conducting vias,” they also serve an additional purpose of mechanically holding this three layer textile surface together. Since the EBG textile ground plane is semi-flexible, it can conform to the surface of the fuselage of an aircraft. The EBG ground plane presents high impedance to the “creeping” surface waves propagating on the fuselage of the aircraft and is, thus, able to suppress antenna backlobes created by them over the frequencies within this “band gap.” The filter characteristics of this EBG surface is determined by several parameters [4]: the size of the conducting square patch of the top layer, the diameter of the central conducting post, and the thickness and dielectric constant of the dielectric textile layer. The frequency characteristics of the surface-wave band gap was measured by locating two wideband ridge waveguide horn antennas, one on either side of the EBG surface and measuring its S_{11} transmission properties using a network analyzer. A picture of this experimental set-up is shown in Figure 14; the measured surface-wave band gap for one the earlier EBG textile ground planes is shown in Figure 15. Notice that the surface wave cut off starts at 1.57 GHz and continues for a wider band of frequencies above it. The measured attenuation of TM type surface waves by the 14" square EBG ground plane at 1.5754 GHz is 27.5 dB.

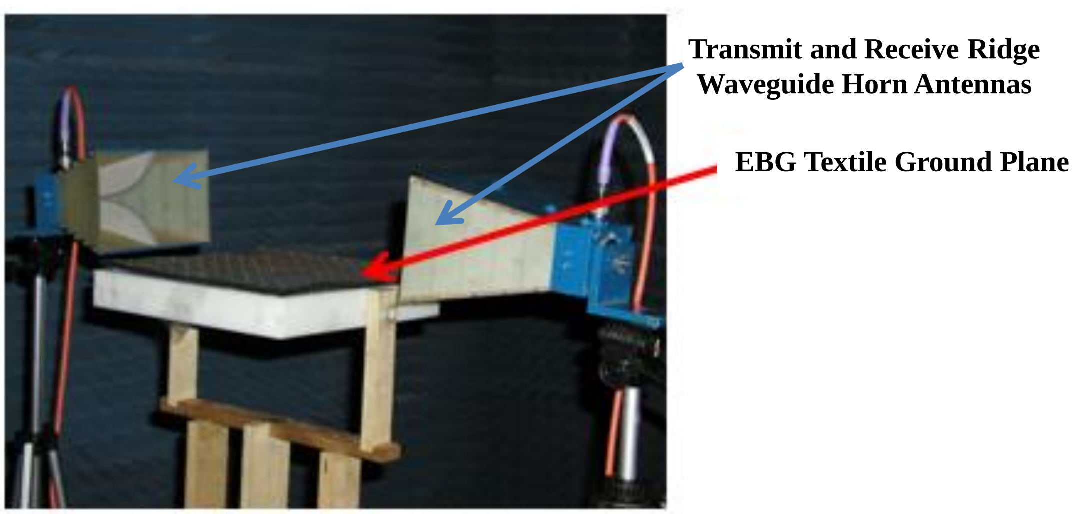

Figure 14. Measurement of the Surface Wave Frequency Band Gap of the Electronic Band Gap (EBG) Textile Ground Plane

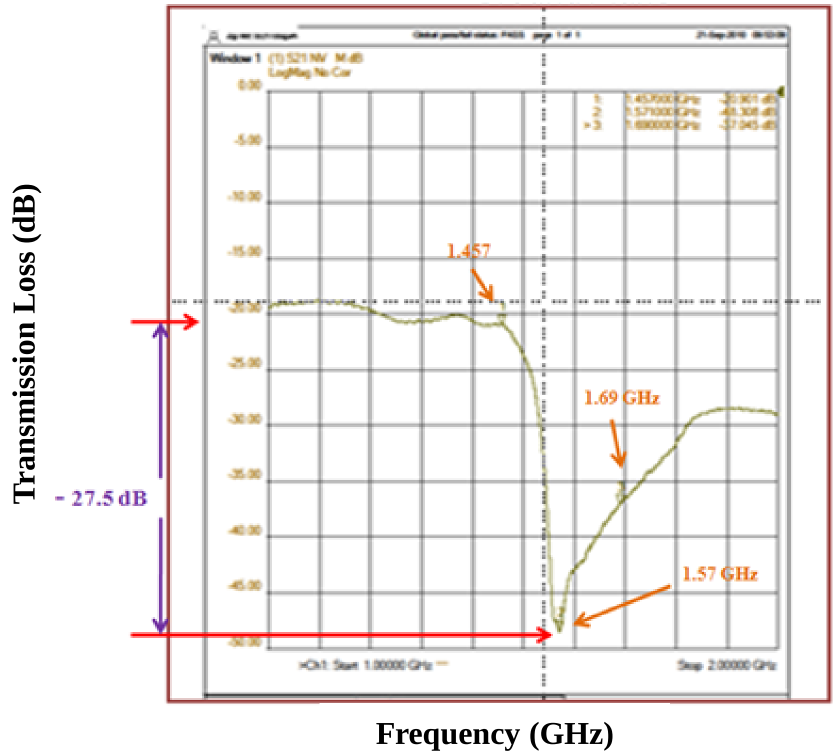

Figure 15. Measured Attenuation versus Frequency of TM Type Surface Waves on a Metal Surface by the EBG Ground Plane versus Frequency; the Band Gap Starts at 1.57 GHz

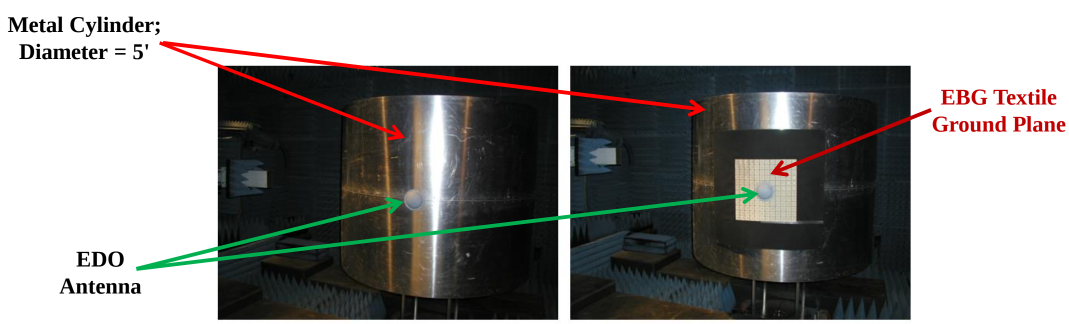

Figure 16 (a) **Figure 16 (b)**

Figure16. EDO Antenna Placed on the Bare Metal Cylinder [Figure 16(a)] and on the Metal Cylinder Covered by the EBG Ground Plane [Figure 16(b)] to Verify Suppression of Antenna Backlobes

Figure 16 shows a picture of the EDO antenna (Model C146-24-1) placed on top of a large metal cylinder that simulates the fuselage of an aircraft; the cylinder had a diameter of 5'. The roll plane antenna pattern was measured in MITRE's Near Field Antenna range using cylindrical scanning. The pattern was first measured by placing the antenna directly on the surface of bare cylinder without the EBG ground plane, as shown in Figure 16(a) on the left, to demonstrate the effect of curved surface diffraction of the antenna backlobes. The measured roll plane RHCP pattern for this case is shown in

Figure 17 and shows a very significant and wide backlobe in the radiation pattern. The EBG textile ground plane was then draped around the top surface of the cylinder and the EDO antenna was then placed at the center of the ground plane as shown in Figure 16(b) on the right side of this figure. The measured roll plane pattern for this second case is also shown in Figure 17 for comparison.

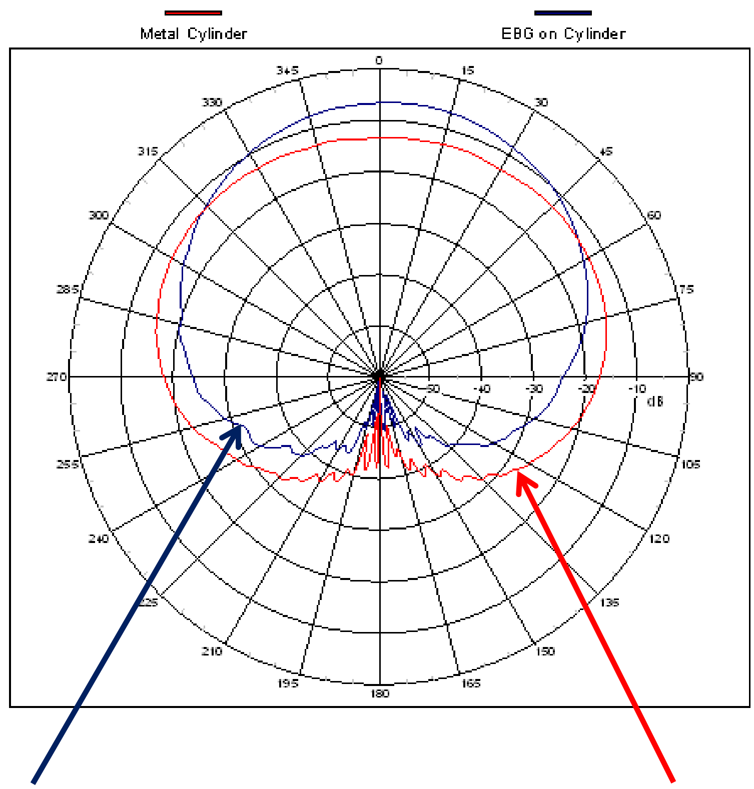

EBG Ground Plane on Metal Cylinder **Bare Metal Cylinder**

Figure 17. Comparison of the Measured RHCP Roll Plane Patterns of an EDO Antenna Measured on 5' Diameter Bare Metal Cylinder and with EBG Ground Plane on the Cylinder

It can be seen that the EBG does reduce the backlobes compared to the previous case. The gain at zenith also increases by more than 5 dB. The radiated energy from lower elevation is diverted towards the zenith direction increasing the gain around zenith by almost 4 dB. The achieved reduction in the backlobe level is not large enough indicating the surface wave attenuation by the EBG ground plane is not adequate to achieve a significant suppression of backlobe radiation level. The EDO antenna was then replaced by a Reduced Surface Wave (RSW) microstrip annular ring patch antenna resonant at 1.5754 GHz; the inner periphery of this antenna is connected to the ground plane – hence, it is also called a “Shorted Annular Ring” patch antenna. The RSW antenna was first placed on the surface of bare metal cylinder as shown in Figure 18(a); its RHCP roll plane pattern was measured using cylindrical scanning as previously. The measured pattern is shown in Figure 19. Notice the RSW is able to suppress the surface wave backlobes much better than the EDO antenna shown in the previous figure. However, it is not able to completely suppress all backlobe radiation which was the desired goal of this study. Next the RSW antenna was used in conjunction with the EBG textile ground plane. The EBG ground plane was placed on the metal cylinder and the RSW antenna was placed on top of it as shown in Figure 18(b). The roll plane RHCP pattern was measured and is shown in Figure 19. The left-right asymmetry in the pattern noticed for the bare metal cylinder may be due to a misalignment of the RSW antenna when placed on the cylinder during these measurements. The combination of RSW antenna with the EBG ground plane is able to achieve the best suppression of backlobe radiation from the antenna of all cases considered until now.

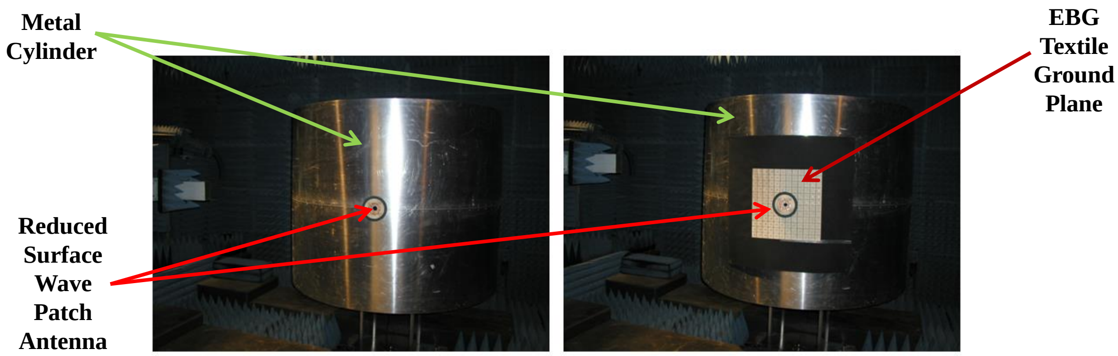

Figure 18(a)   **Figure 18(b)**

Figure 18. Reduced Surface Wave (RSW) Microstrip Shorted Annular Ring Antenna Placed on the Large Metal Cylinder – without the EBG Ground Plane [shown in Figure 18(a)] and with the EBG Ground Plane [shown in Figure 18(b)]

The conclusion obtained from the second part of these investigations is that the EBG ground plane does not provide enough attenuation to reduce the backlobe level to a level low enough to assure the best protection against multipath and interference for GPS antennas. However, when used in conjunction with a RSW antenna the reduction in surface wave diffraction is large enough to reduce these backlobe levels to a negligibly low level to assure good protection against multipath and interference effects – especially co-site interference from radiation from other transmitting antenna located on the belly of the aircraft such as harmonic radiation from VHF and UHF antennas or other L band communications antennas.

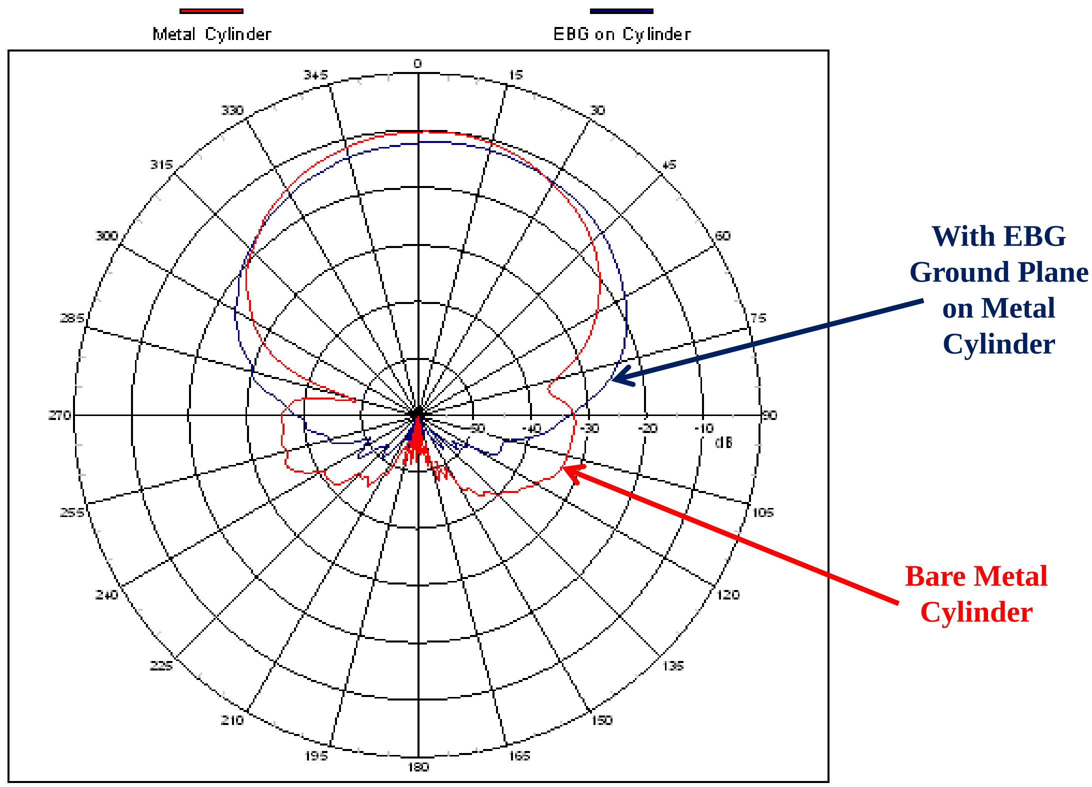

Figure 19. Comparison of the Measured Roll Plane RHCP Radiation Patterns of the RSW Textile Antenna Placed on the Bare Metal Cylinder and on the EBG Ground Plane placed on the Metal Cylinder

References

1. Rama Rao B., E. N. Rosario, and R. J. Davis, April 2006, "Radiation Pattern Analysis of Aircraft Mounted GPS Antennas and Verification Through Scale Model Testing," *Proceedings 2006 IEEE PLANS Conference*, San Diego, California.

2. Avloni J. (Eeonyx Corporation), November 5, 2010, "Textiles Coated with Electrically Conductive Formulations and Their Applications," International Conference on Textile Coating and Laminating, Cannes, France.

3. Rama Rao B., M. N. Solomon, et al., September 1998, "Research on GPS Antennas at MITRE," *Proceedings IEEE Position Location and Navigation Symposium*, Palm Springs, California, pp. 634-661.

4. Sievenpiper D., L. Zhang, R. Broas, N. Alexopoulos, and E. Yablonovich, November 1999, "High Impedance Electromagnetic Surfaces with a Forbidden Frequency Band," *IEEE Transactions on Microwave Theory and Techniques*, Vol. 47, pp. 2059-2074.

5. Long Li, Q. Chen, Q. Yuan, et al., 2008, “Surface-Wave Suppression Band Gap and Plane-Wave Reflection Phase Band of Mushroomlike Photonic Band Gap Structures,” *Journal of Applied Physics*, Vol. 103, 023513.

6. Baggen R., et al., March 2008, “Low Profile Galileo Antenna Using EBG Technology,” *IEEE Transactions on Antennas and Propagation*, Vol. 56, No. 3, pp. 667-674.

7. McKinzie W. E., R. Hurtado, W. Klimczak, January 28-30, 2002 “Artificial Magnetic Conductor Technology Reduces, Size and Weight for Precision GPS Antennas,” *Proceedings Institute of Navigation Technical Meeting*, San Diego, California, pp. 1-12.